Journal of Applied Polymer Science

Preparation of Poly(methyl methacrylate)-Grafted Attapulgite by Surface-Initiated Radical Polymerization

Haicun Yang,[1] Hongting Pu,[1] Fanghong Gong[2]

[1]Institute of Functional Polymers, School of Materials Science and Engineering, Tongji University, Shanghai 201804, China
[2]College of Materials Science and Engineering, Changzhou University, Changzhou 213164, China
Correspondence to: H. Pu (E-mail: puhongting@tongji.edu.cn) and F. Gong (E-mail: fhgong@cczu.edu.cn)

ABSTRACT: Poly(methyl methacrylate) (PMMA) was bonded on the surface of attapulgite (ATP) by using an ammonium persulfate amine redox initiation system via grafting from approach. ATP was modified with (3-aminopropyl)triethoxysilane to anchor amine groups on the surface, and then the amine-functionalized ATP was further treated with methacryloyl chloride and 4,4′-azobis(4-cyanovaleric acid) to give methacryl- and azo-functionalized ATP, respectively. Subsequently, surface-initiated graft polymerization of MMA in a soap-free emulsion was performed to afford ATP/PMMA hybrids. Meanwhile, graft polymerizations on the surface of methacryl- and azo-functionalized ATP were carried out for comparison. The grafting of PMMA on the surface of ATP was characterized by Fourier transform infrared spectroscopy, X-ray photoelectron spectroscopy, and thermogravimetric analysis (TGA). The crystal structure of hybrids was characterized by X-ray diffraction analysis. The morphology of hybrids was observed by scanning electron microscopy and transmission electron microscopy. The degree of grafting obtained from surface-initiated graft polymerization in a soap-free emulsion was found to be the greatest (29.4%) estimated from TGA. © 2014 Wiley Periodicals, Inc. J. Appl. Polym. Sci. **2014**, *131*, 41062.

KEYWORDS: clay; grafting; radical polymerization

Received 27 February 2014; accepted 25 May 2014
DOI: 10.1002/app.41062

INTRODUCTION

In the recent years, the synthesis of hybrid organic–inorganic nanocomposites is attracting considerable attention because of their significant promise for a variety of potential applications in electro-optical modulator,[1] special engineering plastic,[2] catalytic,[3] biological materials,[4] and so forth. There are a large number of techniques available for the synthesis of functionalized hybrid nanocomposites with multiple-layered morphology, and these techniques include active free radical graft polymerization,[5] shell crosslinked polymer micelles,[6] and graft via self-assembling.[7]

Covalent attachment of polymer chains by a chemical reaction has been widely used for the synthesis of hybrid organic–inorganic nanocomposites. The immobilization of the polymer chains chemically attached to a solid surface can be introduced by performing "click chemistry" with polymerization.[8] It includes three means "grafting to," "grafting through," and "grafting from" methods with different mechanisms.[9–11] According to the grafting to method, the chemical bonds can be constructed by a chemical reaction of the intrinsic or complementary active functional groups on the particles surface with reactive end groups of end-functional polymer chains, which is also called "coupling grafting." Although the mechanism of this method is simple, it possesses some limitations. This approach often suffers from corresponding lower degree of grafting (DG) due to "steric effects."[12] The attaching polymer chains have to overcome the activation barrier that appears as soon as the earlier attached chains begin to overlap, and the steric hindrance for surface tethering enforces along with the increase of DG.[13,14] For the grafting through method, polymerizable functional groups are anchored on the surface of particles first, and then the copolymerization of the polymerizable particles and the monomer was applied. In this process, the decomposition of initiator generates original free radicals, and then these initiator free radicals initiate monomer to form the monomer free radicals and polymer free radicals. Only when these kinds of free radicals diffuse to the surface of particles, functionalized particles are made to take part in copolymerization to form the graft polymer chains via a grafting through method. This approach still possesses an unsatisfactory DG due to the "microinhomogeneity" in the heterogeneous system.[15]

For the grafting from method, the surface of nanoparticles is designed to bear initiated groups first, and then the subsequent *in situ* polymerization is used. This approach is also known as "surface-initiated graft polymerization."[16] Recently, a variety of controlled living radical polymerization techniques have been

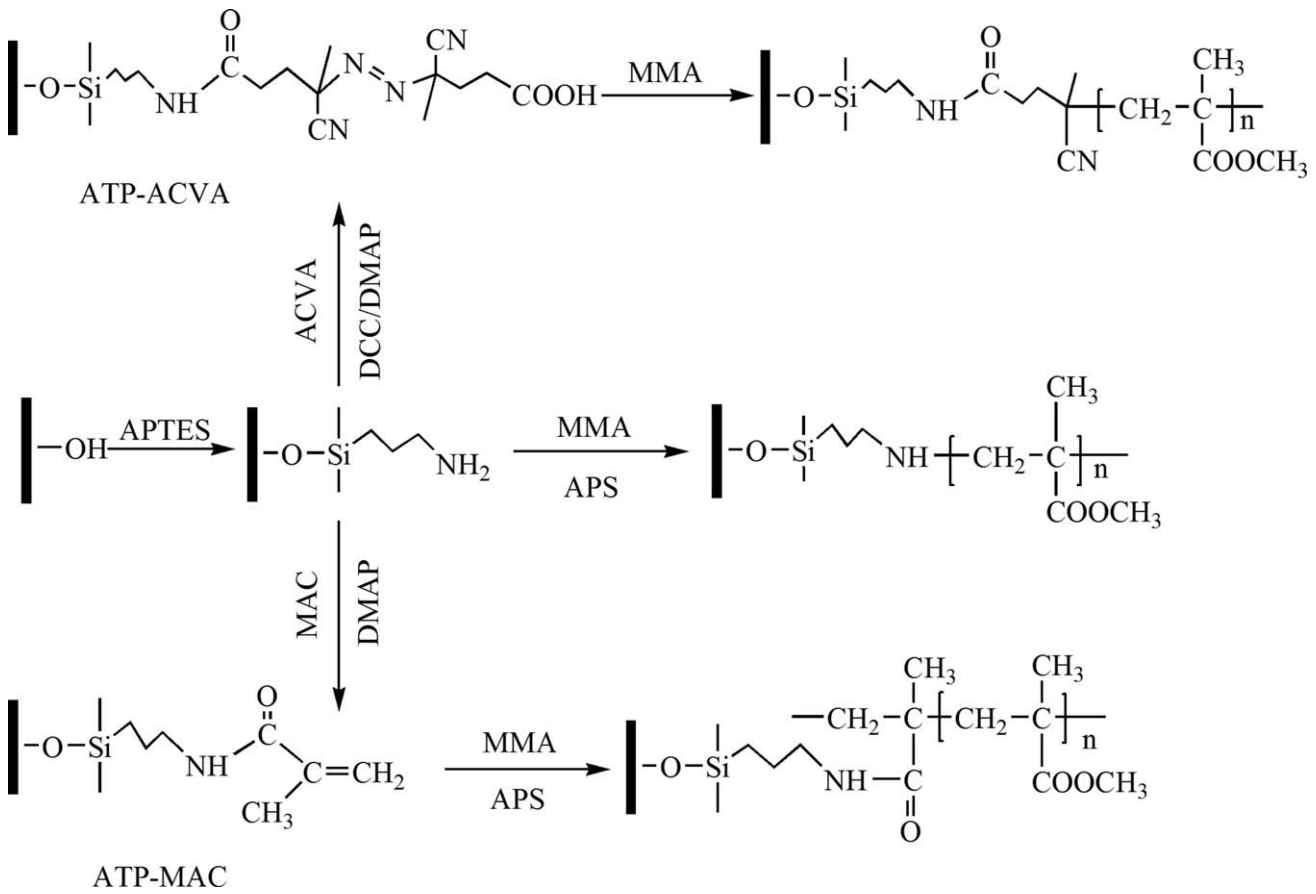

Scheme 1. Schematic of experimental design.

developed rapidly for modifying the surface of nanoparticles with organic polymers, such as atom transfer radical polymerization,[17] nitroxide-mediated polymerization,[18] and reversible addition-fragmentation chain transfer polymerization.[19] These methods provide some advantages such as grafted polymer with controlled molecular weight and narrow polydispersity. However, the condition of most surface-initiated living polymerization on the surface of nanoparticles is usually stringent, and this application is challenging.

Although the grafting from approach provides higher DG because of the chain growth is realized by the diffusion of monomer,[20,21] it requires several steps to attach initiated groups on the surface of particles, and in which, these surface-anchored initiators are of lower activity.[22,23] On the other hand, a very efficient method of generating free radicals under mild condition is by one-electron transfer reaction, the most effective of which is a redox initiation consisting of the electron donor and acceptor.[24] Silane chemistry has been extensively applied in the surface modification of inorganic particles.[25–27] Thus, instead of attaching initiated groups on the surface of particles, surface-bonded reducing groups such as amine, mercaptan, and aromatic tertiary amine groups can also initiate polymerization in the presence of oxidizing initiator.[28–30] Similar reports of surface-initiated graft polymerization on inorganic oxide such as SiO_2, TiO, and ZnO have been disclosed.[31–33] However, to our knowledge, relatively less research about attapulgite (ATP) surface modification via surface-initiated graft polymerization has been carried out. In this research, poly(methyl methacrylate) (PMMA) was bonded onto the surface via three facile graft polymerizations as shown in Scheme 1. Amine, azo, and methacryl groups were introduced covalently onto the surface of ATP particles first, and then graft polymerizations were carried out to prepare ATP-*g*-PMMA hybrids according to different kinds of mechanisms. The grafting of PMMA on the surface of ATP was characterized using Fourier transform infrared (FTIR) spectroscopy, thermogravimetric analysis (TGA), X-ray photoelectron spectroscopy (XPS), X-ray diffraction (XRD), scanning electron microscopy (SEM), and transmission electron microscopy (TEM). The DG of three methods was compared, and the effect of polymerization condition on DG of grafting from a method based on the redox initiation is mainly investigated.

EXPERIMENTAL

Materials

ATP was obtained from Jiuchuan Nano-Material Science, Jiangsu, China. It was activated with hydrochloric acid of

1 mol/L and then dried in a vacuum oven at 120°C for 36 h before use. MMA (Shanghai Chemical Factory, China) was passed through a column of basic alumina to remove inhibitors, then distilled under reduced pressure, and stored in an argon atmosphere at −5°C. (3-Aminopropyl)triethoxysilane (APTES), 4-dimethylaminopyridine (DMAP), *N*,*N*′-dicyclohexylcarbodiimide (DCC), 4,4′-azobis(4-cyanovaleric acid) (ACVA), and methacryloyl chloride (MAC) were all of analytical grade received from Aladdin Reagent, Shanghai, China. Ammonium persulfate (APS) and all solvents were of analytical grade and used as received from Sinopharm Chemical Reagent, Shanghai, China.

Anchoring of Amine Groups Onto Attapulgite (ATP-NH_2)

The ATP-NH_2 was prepared by a silanization reaction according to the method reported previously.[34] In a typical procedure, 4 g of activated ATP was dispersed in 150 mL of xylene in a 250-mL round-bottomed flask, and the mixture was ultrasonicated for 60 min to obtain a homogeneous dispersion, to which 8 mL of APTES was added. The reaction mixture was maintained at reflux for 10 h with a strong mechanical stirring. After the reaction, the mixture was filtered, and the sediment was washed several times with ethanol to remove unreacted APTES. The resulting ATP-NH_2 was dried in a vacuum oven at 50°C. The amount of primary amine groups of unit mass was 1.63 mmol/g calculated by the elemental analysis.

Anchoring of Methacryl Groups Onto Attapulgite (ATP-MAC)

To prepare ATP-MAC particles, 1 g of ATP-NH_2 was suspended in 100 mL dichloromethane under the condition of ultrasonic vibration. Then, 4 mL of MAC, 5 g of DMAP as acid-binding agent, and trace of CuCl as polymerization retarder were added into ATP-NH_2 suspension. The amidation reaction was carried out with a magnetic stirring bar at room temperature for 4 h under nitrogen protection. After the reaction, the mixture was centrifuged and washed several times with DMF. The resulting ATP-MAC particles were dried in a vacuum oven at room temperature. The amount of methacryl groups of unit mass was 0.67 mmol/g calculated by the elemental analysis.

Immobilization of Azo Groups Onto Attapulgite (ATP-ACVA)

The ATP surface anchoring of azo groups was as follows: 1 g of ATP-NH_2 was dispersed in 75 mL ethyl acetate under the condition of ultrasonic vibration, and 3 g of ACVA was dissolved in 75 mL ethyl acetate with insufflating nitrogen for 20 min, to which 1.44 g of DCC as condensation agent and catalytic amount of DMAP were added. After stirring for 20 min, ATP-NH_2 dispersion was added to the solution. The amidation reaction was carried out with a magnetic stirrer at 30°C for 12 h under nitrogen atmosphere. After the reaction, the mixture was centrifuged and washed with isopropanol for several times, and the final precipitate ATP-ACVA was dried in a vacuum oven at room temperature. The amount of azo groups of unit mass was 0.42 mmol/g calculated by the elemental analysis.

Preparation of ATP-g-PMMA Hybrids

The preparation of ATP-*g*-PMMA using ATP-NH_2, ATP-MAC, and ATP-ACVA was performed at the condition of soap-free emulsion polymerization. A typical procedure was as follows: 0.5 g of ATP-NH_2, 1.2 g of ATP-MAC, and 1.9 g of ATP-ACVA were suspended in 9 g of MMA, and these mixtures were ultrasonicated for 5 min. Samples thus obtained were then mixed with 150 mL distilled water. After stirring vigorously for 10 min under the condition of ultrasonic vibration, 0.9 g of APS was added to ATP-NH_2 and ATP-MAC systems. The subsequent polymerizations were carried out under N_2 protection in an oil bath at 65°C and maintained for the required time. After the reaction, the solid products were centrifuged, washed, and extracted with THF for 24 h by Soxhlet extraction method. Finally, the resulting ATP-*g*-PMMA was dried in a vacuum oven at 50°C.

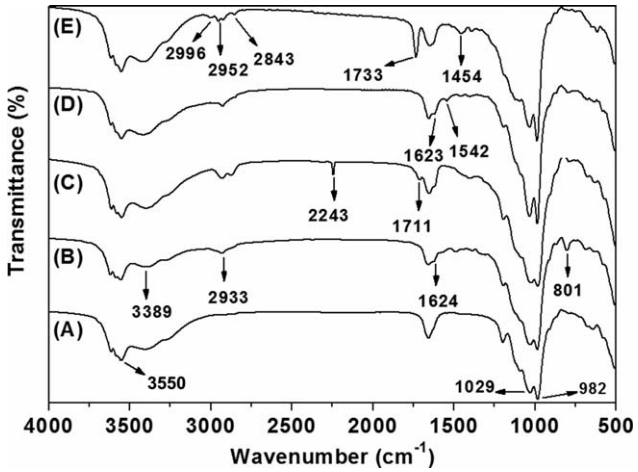

Figure 1. FTIR spectra of (A) ATP, (B) ATP-NH_2, (C) ATP-ACVA, (D) ATP-MAC, and (E) ATP-*g*-PMMA.

Characterization

Changes in the surface chemical bonds of ATP-NH_2, ATP-ACVA, ATP-MAC, and ATP-*g*-PMMA were analyzed by FTIR spectroscopy using Avatar 370 FTIR Spectrometer (USA) in the frequency range of 500–4000 cm^{-1}. XPS measurement was carried out using a Thermo Fisher Escalab 250Xi X-ray photoelectron spectrometer (USA) in an ultrahigh vacuum with Al Kα radiation. The XRD experiment was carried out on a Rigaku 18 kW rotating anode X-ray generator (Japan) with Cu Kα radiation operated at 40 kV and 100 mA. SEM photographs were taken on a Zeiss SUPRA55 SEM (Germany) with an accelerated voltage of 5 kV. TEM was carried out by a JEM-1200 EX/S TEM (Japan) with an accelerating voltage of 200 kV. For TEM measurement, the dried particles were dispersed in THF with an ultrasonic vibration for 20 min and then deposited on a copper grid covered with a perforated carbon film. TGA was carried out using a Netzsch TG209 F3 system (Germany) within the temperature range of 50–850°C at a heating-up rate of 10°C/min under a continuous nitrogen flow.

RESULTS AND DISCUSSION

Preparation and Characterization of ATP-g-PMMA Hybrids

FTIR Analysis. The FTIR spectra of ATP, ATP-NH_2, ATP-ACVA, ATP-MAC, and ATP-*g*-PMMA are shown in Figure 1. The spectrum of ATP (Figure 1, Curve A) exhibits two Si—O stretching vibrations at 982 and 1029 cm^{-1}. The absorption peak at 3550 cm^{-1} is attributed to —OH stretching vibrations. In contrast to that of ATP, in the FTIR spectrum of ATP-NH_2

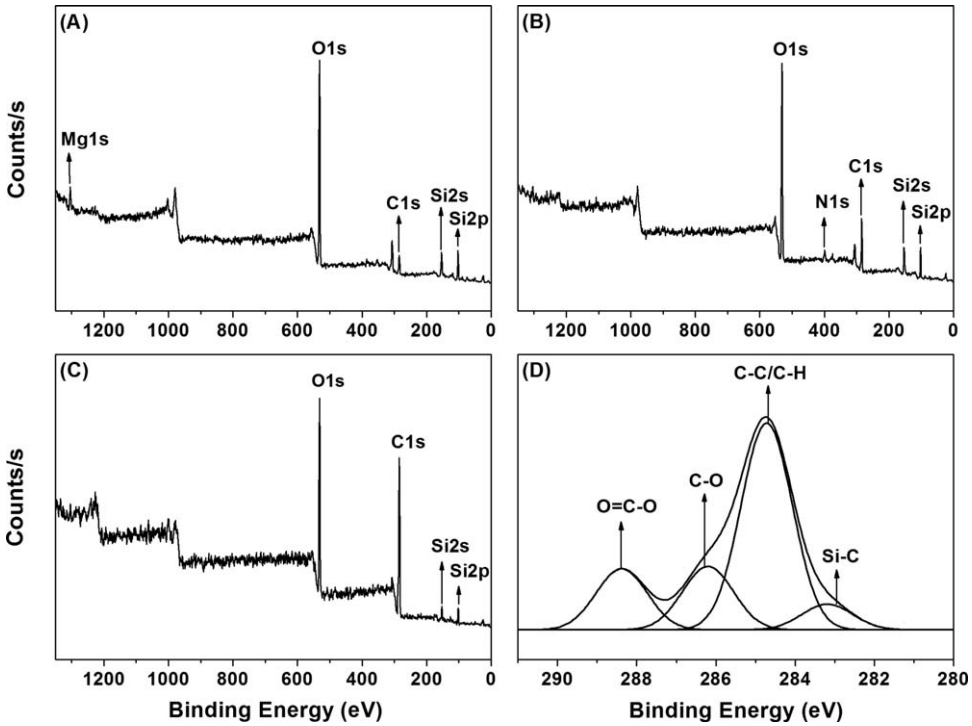

Figure 2. XPS full-scan spectrum of (A) ATP, (B) ATP-NH_2, (C) ATP-*g*-PMMA, and (D) C1s core-level spectra of ATP-*g*-PMMA.

(Figure 1, Curve B), the peak at 801 cm^{-1} is attributed to N—H in-plane bending vibration. Influenced by the peak at 1640 cm^{-1} of H—O—H of ATP, a weak overlapped peak at 1624 cm^{-1} attributed to N—H out-of-plane is observed. The presence of the anchored propyl group is confirmed by the C—H stretching vibration appearing at 2933 cm^{-1}. Besides, a wide peak observed at 3389 cm^{-1} is attributed to the overlapping band of N—H stretching vibration and associated Si—O—H. For ATP-ACVA (Figure 1, Curve C), the band at 2243 cm^{-1} was attributed to C≡N stretching vibration, and the peak at 1711 cm^{-1} is assigned to C═O stretching derived from unreacted carboxyl of ACVA. In the spectrum of ATP-MAC (Figure 1, Curve D), peaks at 1542 and 1623 cm^{-1} corresponded with C═C and CONH are observed. All these changes suggest that APTES, ACVA, and MAC have been successfully grafted on the surface of ATP. The PMMA-grafted ATP is confirmed by the presence of a new strong peak at 1733 cm^{-1} assigned to the C═O stretching vibration of PMMA (Figure 1, Curve E), and significantly enhanced characteristic stretching bands of alkyl chains at 2996, 2952, 2843, and 1454 cm^{-1} can be observed in the FTIR spectrum of ATP-*g*-PMMA when compared with the others. All of these results unanimously interpret that PMMA was anchored on the surface of ATP successfully.

XPS Analysis. XPS was used to investigate the surface chemical composition. Figure 2 shows the XPS spectrum of ATP, ATP-NH_2, and ATP-*g*-PMMA. The wide-scan spectrum of ATP [Figure 2(A)] is dominated by signals attributable to silicon (103.3 eV, Si2p; 154.4 eV, Si2s), magnesium (1304.4 eV, Mg1s), carbon (284.9 eV, C1s), and oxygen (531.8eV, O1s) elements. In the spectrum of ATP-NH_2 [Figure 2(B)], a weak but clearly visible peak of nitrogen (399.2 eV, N1s) confirms the anchoring of APTES on the surface of ATP. On grafting of PMMA [Figure 2(C)], the C1s peak shows an increased intensity than ATP and ATP-NH_2, indicating that PMMA chains are grafted from the surface of ATP. The C1s core-level spectrum of ATP-*g*-PMMA can be curve-fitted with four peak components having binding energy at 283.2, 284.7, 286.2, and 288.4 eV attributable to the Si—C, C—C/C—H, C—O, and O═C—O, respectively [Figure 2(D)].

XRD Analysis. The crystal structures of ATP, ATP-NH_2, and ATP-*g*-PMMA were investigated by XRD analysis. The XRD

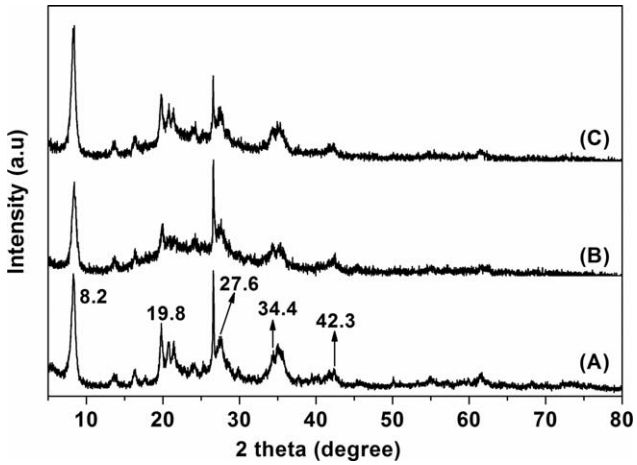

Figure 3. XRD patterns of (A) ATP, (B) ATP-NH_2, and (C) ATP-*g*-PMMA.

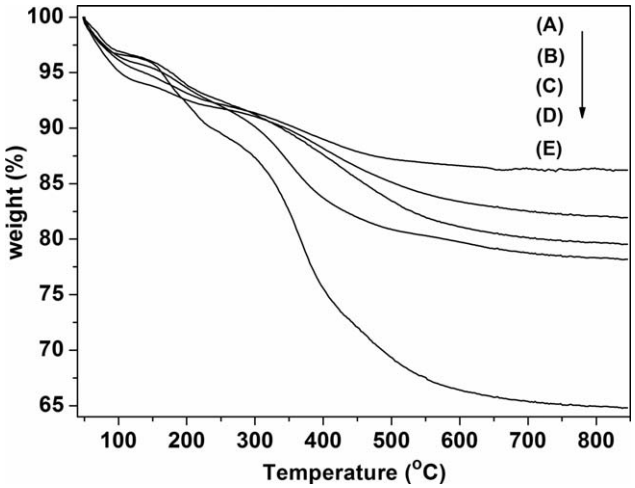

Figure 4. TGA spectra of (A) ATP, (B) ATP-NH_2, (C) ATP-ACVA, (D) ATP-MAC, and (E) ATP-*g*-PMMA.

patterns in the 2θ range 5°–80° are presented in Figure 3. The pattern of ATP exhibits several sharp peaks centered at $2\theta = 8.2°$, 19.8°, 27.6°, 34.4,° and 42.3° (Figure 3, Curve A), and these reflection positions are exactly the same for ATP-NH_2 and ATP-*g*-PMMA (Figure 3, Curves B and C). It can be concluded that the surface chemical graft polymerization has no effect on the crystal structure of ATP.

Thermogravimetric Analysis. The TGA results of ATP, ATP-NH_2, ATP-MAC, ATP-ACVA, and ATP-*g*-PMMA are shown in Figure 4, and the common analysis method for inorganic particles grafted polymer is used.[35] It is observed that ATP loses 13.63% of the total weight attributed to absorbed water, zeolite water, crystal water, and constitutional water (Figure 4, Curve A). After the surface anchoring of APTES, ACVA, and MAC, the total weight loss attains to 16.8%, 19.4%, and 20.8% respectively (Figure 4, Curves B–D). The TGA curve of ATP-*g*-PMMA shows a major decomposition at the temperature range from 260 to 550°C, indicating the surface grafting of ATP by PMMA (Figure 4, Curve E). When compared with ATP-NH_2, the TGA curves of ATP-*g*-PMMA show a total loss weight of 34.2%, which indicated that the DG of PMMA grafted from ATP-NH_2 was 18.4%. DG of other ATP-*g*-PMMA hybrids is estimated by this method. The TGA analysis suggests a successful graft polymerization on the surface of ATP initiated by a redox initiation system.

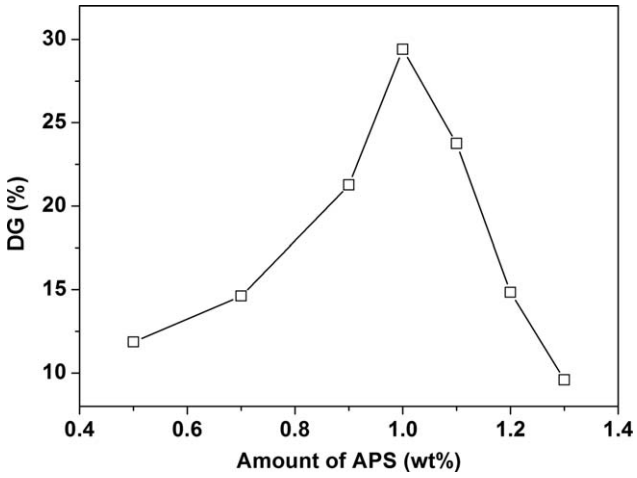

Figure 6. The effect of the amount of APS on DG.

Comparison of Degree of Grafting for Three Approaches

The variation of DG with time for three approaches is shown in Figure 5. It can be observed that there is a remarkable difference in DG. When ATP-NH_2 is used, the hybrids are synthesized by grafting from method based on a redox initiation system. DG increases with lengthening reaction time then levels off after 10 h and achieves its stationary value of ~ 29.4%. However, when ATP-ACVA is used, DG is merely 21.8%. In the radical graft polymerization initiated by azo groups introduced onto the surface, the decomposition of surface azo groups proceeds gradually, and DG increases with progress of the polymerization time and levels off after 8 h. The reason is that radicals formed on the surface at the initial stage of polymerization can initiate graft polymerization, whereas at the final stage, radicals formed

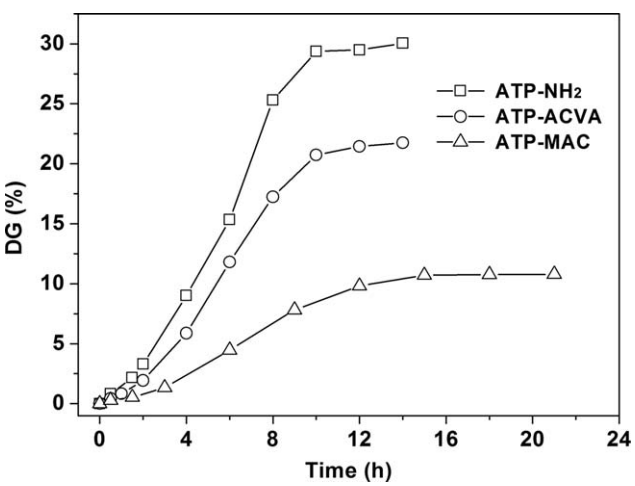

Figure 5. Variation curves of DG with time for three approaches.

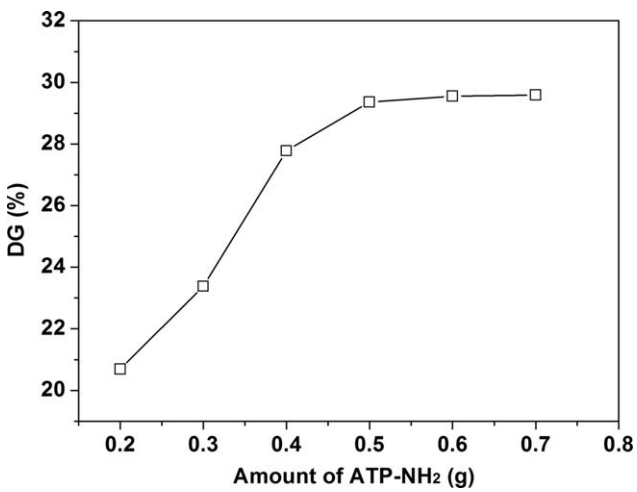

Figure 7. The effect of the amount of ATP-NH_2 on DG.

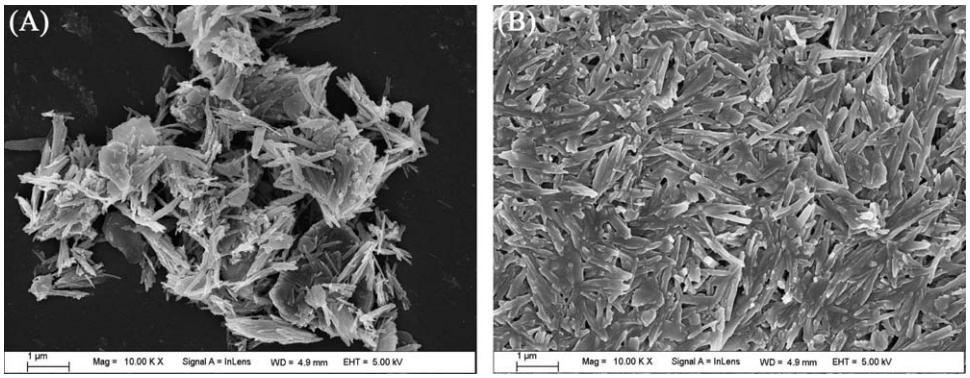

Figure 8. SEM images of (A) ATP and (B) ATP-*g*-PMMA hybrids.

on the surface cannot initiate polymerization because the growing polymer radical from the surface and grafted polymer chains block the diffusion of monomer to the surface.[36] In addition, a large number of one-end anchored ACVA generate free radicals and lead to ungrafted polymer, resulting in the termination of graft polymerization. When using ATP-MAC, the grafted polymer chains grow via a grafting through method; it is obvious that DG was less satisfactory than grafting from method. Generally, the expected steric hindrance originating from the growing polymer radical from the surface and grafted polymer chains exists in all these approaches. The highest DG of ATP-NH_2 may be due to the fact that the activation energy in generating free radicals by redox initiation is considerably lower than that of azo groups. However, the inevitable steric hindrance and homopolymerization involved in the graft polymerization result in the limitation of DG.

Effects of Polymerization Condition on Degree of Grafting of Surface-Initiated Graft Polymerization in a Soap-Free Emulsion

Two kinds of nucleation mechanisms existed synchronously in the redox initiation system. The polymerization condition has an influence on polymerization rate and DG. A lower polymerization temperature (65°C) was chosen as the suitable temperature to inhibit the homopolymerization to some extent, and to obtain a stable emulsion, oil–water ratio of 6 wt % was selected.

First, by fixing the feed ratio of ATP-NH_2/MMA (0.5/9), the effect of the amount of APS (weight percentage of MMA) is taken into account, and the result is demonstrated in Figure 6. It can be seen that DG increases with the increase of the amount of APS and reaches its utmost value when the amount of APS is 1 wt %, then declines as the amount of APS is over 1 wt %. The graft polymerization rate is extremely slow because of the small amount of APS. When increasing the amount of APS, the redox initiation reaction is accelerated, and thus, the graft polymerization is sped up greatly, resulting in an enhancement of DG. However, graft polymerization is carried out exceedingly rapidly as an excessive amount of APS, which leads to the rapid formation of compact polymer blocking layer and the premature termination of graft polymerization. Besides, the excessive amount of APS also accelerates the homopolymerization. The homopolymer primary micelles form prematurely and consume certain proportion of monomers, which decreases the monomer amount for the graft polymerization and leads to a lower DG.

Subsequently, by fixing the feed ratio of APS/MMA (0.09/9), the effect of the amount of AT-NH_2 on DG is considered. It can be seen from Figure 7 that DG increases with increasing AT-NH_2 content when the amount of AT-NH_2 is less than 0.5 g. This is attributed to the fact that redox reaction rate is extremely slow when less amount of ATP-NH_2 is used, and thermal decomposition is the main consumption method of

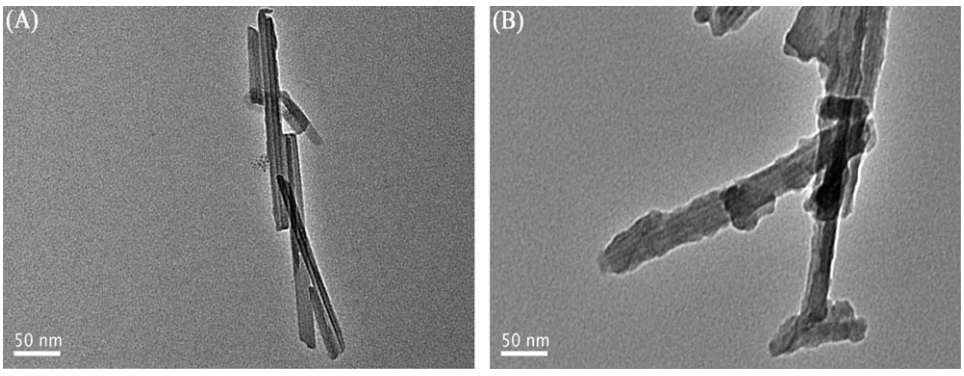

Figure 9. TEM images of (A) ATP and (B) ATP-*g*-PMMA hybrids.

APS. The percentage of APS that involves in redox initiation reaction is declined, and ATP-*g*-PMMA hybrids are embedded in the ungrafted polymer layer at a lower DG. The graft polymerization rate is accelerated with increasing the amount of AT-NH_2, which results in the increase of DG. As the amount of AT-NH_2 exceeds 0.5 g, the DG levels off at approximately 29.4%. The reason is that APS reacts with primary amine groups on the surface of ATP-NH_2 to generate anchored radicals. The amount of primary amine groups of unit mass is fixed, and each grafting chain can attain to its saturate polymerization degree. Consequently, the amount of anchored polymer of unit mass is fixed accordingly, which leads to the maximum value of DG.

Morphology Analysis of ATP-g-PMMA Hybrids

SEM micrographs of ATP and ATP-*g*-PMMA are shown in Figure 8. Figure 8(A) shows the virgulate morphology of ATP, and a number of large agglomerates can be observed because of the strong surface polarity that results from the hydroxyl groups on the external surface of ATP. As seen in Figure 8(B), the agglomeration was alleviated obviously after surface grafting. Figure 9 shows the TEM pictures of ATP and ATP-*g*-PMMA. A relatively smooth surface of ATP rod is observed in Figure 9(A), and its diameter is about 25 nm. It can be seen from Figure 9(B) that the diameter of ATP-*g*-PMMA is around 40–50 nm, and a remarkable change of surface morphology can be observed after surface grafting of PMMA. The TEM pictures can be considered as the direct evidence that ATP-*g*-PMMA hybrids were prepared successfully.

CONCLUSIONS

In this study, three facile syntheses of PMMA anchored on the surface of ATP were carried out successfully, and the DG was compared. The surface grafting of ATP by PMMA was confirmed by FTIR, XPS, and TGA analyses. The crystal structure of ATP-*g*-PMMA was investigated by XRD analysis. The morphologies of PMMA-grafted ATP were ascertained by SEM and TEM. The TGA analysis revealed that the graft polymerization initiated by a redox initiation system exhibited the highest DG. This grafting from method not only has a feature of high DG but also is feasible and convenient because the surface modification of ATP via organic silicon is easy to be achieved. For the surface-initiated graft polymerization in a soap-free emulsion under the optimal condition, free radicals were created on the surface of ATP-NH_2 via redox initiation reaction, and graft polymerization occupied the main role than that of homopolymerization, which resulted in a high DG of 29.4%. Surface graft polymerization had no effect on the crystal structure of ATP. The morphology of ATP was changed after surface grafting of PMMA.

ACKNOWLEDGMENTS

This work was financially supported by the project funded by the Priority Academic Program Development (PAPD) of Jiangsu Higher Education Institutions.

REFERENCES

1. Chen, C. M. *IEEE J. Quantum. Elect.* **2012**, *48*, 61.
2. Sanchez, C.; Julián, B.; Belleville, P.; Popall, M. *J. Mater. Chem.* **2005**, *15*, 3559.
3. Sharma, R. K.; Gulati, S.; Pandey, A.; Adholeya, A. *Appl. Catal. B: Environ.* **2012**, *125*, 247.
4. Kadib, A. E. I.; Bousmina, M. *Chem.—Eur. J.* **2012**, *18*, 8264.
5. Zhu, J.; Zhang, G.; Shao, K.; Zhao, C. J.; Li, H. T.; Zhang, Y.; Han, M. M.; Lin, H. D.; Na, H. *J. Power Sources* **2011**, *196*, 5803.
6. Zhang, X. H.; Chen, H. C.; Ma, Y. H.; Zhao, C. W.; Yang, W. T. *Appl. Surf. Sci.* **2013**, *27*, 121.
7. Zhang, W. A.; Müller, A. H. E. *Prog. Polym. Sci.* **2013**, *38*, 1121.
8. Ranjan, R.; Britain, W. J. *Macromolecules* **2007**, *40*, 6217.
9. Zdyko, B.; Luzinov, I. *Macromol. Rapid Commun.* **2011**, *32*, 859.
10. Kalajahi, M. S.; Asl, V. H.; Behboodi-Sadabad, F.; Rahimi-Razin, S.; Roghani-Mamaqani, H. *Polym. Compos.* **2012**, *33*, 215.
11. Bach, L. G.; Islam, M. R.; Seo, S. Y.; Lim, K. T. *J. Appl. Polym. Sci.* **2013**, *127*, 261.
12. Bach, L. G.; Islam, M. R.; Kim, J. T.; Seo, S. Y.; Lim, K. T. *Appl. Surf. Sci.* **2012**, *258*, 2959.
13. Wang, Y. M.; Wang, Y. J.; Lu, X. B. *Polymer* **2008**, *49*, 474.
14. Parnell, A. J.; Martin, S. J.; Dang, C. C.; Geoghegan, M.; Jones, R. A. L.; Crook, C. J.; Howse, J. R.; Ryan, A. J. *Polymer* **2009**, *50*, 1005.
15. Matyjaszewski, K. *Prog. Polym. Sci.* **2005**, *30*, 858.
16. Tsubokawa, N.; Satoh, M. *J. Appl. Polym. Sci.* **1997**, *65*, 2165.
17. Wang, W. C.; Wang, J.; Liao, Y.; Zhang, L. Q.; Cao, B.; Song, G. J.; She, X. L. *J. Appl. Polym. Sci.* **2010**, *117*, 534.
18. Wu, J. R.; Lai, G. Q.; Yu, H. J.; Luo, Z. H. *J. Appl. Polym. Sci.* **2012**, *124*, 3821.
19. Cimen, D.; Caykara, T. *J. Appl. Polym. Sci.* **2013**, *129*, 383.
20. Gromadzki, D.; Makuška, R.; Netopilík, M.; Holler, P.; Lokaj, J.; Janata, M.; Štěpánek, P. *Eur. Polym. J.* **2008**, *44*, 59.
21. Hu, S. W.; Wang, Y.; McGinty, K.; Brittain, W. *J. Eur. Polym. J.* **2006**, *42*, 2053.
22. Prucker, O.; Rühe, J. *Macromolecules* **1998**. *31*, 602.
23. Bachmann, S.; Wang, H. Y.; Albert, K.; Partch, R. J. *J. Colloid Interface Sci.* **2007**, *309*, 169.
24. Sarac, A. S. *Prog. Polym. Sci.* **1999**, *24*, 1149.
25. Wei, B. G.; Chang, Q.; Bao, C. X.; Dai, L.; Zhang, G. Z. *Colloid Surf. A* **2013**, *434*, 276.
26. Sabzi, M.; Mirabedini, S. M.; Zohuriaan-Mehr, J.; Atai, M. *Prog. Org. Coat.* **2009**, *65*, 222.
27. Tomovska, R.; Daniloska, V.; Asua, J. M. *Appl. Surf. Sci.* **2013**, *264*, 670.

28. Ukaji, E.; Furusawa, T.; Sato, M.; Suzuki, N. *Appl. Surf. Sci.* **2007**, *254*, 563.
29. Feng, X. D.; Qiu, K. Y. *Polym. Bull. (China)* **2005**, *4*, 23.
30. Misra, G. S.; Bajpai, U. D. N. *Prog. Polym. Sci.* **1982**, *8*, 61.
31. Zhao, Q.; Tan, T. F.; Qi, P.; Wang, S. R.; Li, X. G.; An, Y.; Liu, Z. *J. Appl. Surf. Sci.* **2011**, *257*, 3499.
32. Tang, E. J.; Fu, C. Y.; Wang, S.; Dong, S. J.; Zhao, F. Q.; Zhao, D. S. *Powder Technol.* **2012**, *218*, 5.
33. Gao, B. J.; Li, D.; Lei, Q. J. *J. Polym. Res.* **2011**, *18*, 1519.
34. Liu, H.; Yang, H. C.; Ye, Q.; Ni, Q. T.; Gong, F. H. *J. Chin. Ceram. Soc. (China)* **2013**, *41*, 848.
35. Ngo, V. G.; Bressy, C.; Leroux, C.; Margaillan, A. *Polymer* **2009**, *50*, 3095.
36. Tsubokawa, N.; Shirai, Y.; Hashimoto, K. *Colloid Polym. Sci.* **1995**, *273*, 1049.